Combined Reconstruction and Registration of Digital Breast Tomosynthesis: Sequential Method versus Iterative Method†

Guang Yang[1], John H. Hipwell[1]
{g.yang,j.hipwell}@cs.ucl.ac.uk

Matthew J. Clarkson[12]
clarkson@drc.ion.ucl.ac.uk

Christine Tanner[13]
tanner@vision.ee.ethz.ch

Thomy Mertzanidou[1]
t.mertzanidou@cs.ucl.ac.uk

Spencer Gunn[4]
spencer.gunn@dexela.com

Sebastien Ourselin, David J. Hawkes, Simon R. Arridge[1]
{s.ourselin,d.hawkes,s.arridge}@cs.ucl.ac.uk

[1] Centre for Medical Image Computing, Department of Computer Science and Medical Physics, University College London (UCL), London, WC1E 6BT, UK

[2] Dementia Research Centre, UCL Institute Of Neurology, London, WC1N 3BG, UK

[3] Computer Vision Laboratory, ETH, 8092, Zürich, CH

[4] Dexela Ltd, London N1 7EU, UK

Abstract

Digital breast tomosynthesis (DBT) has the potential to enhance breast cancer detection by reducing the confounding effect of superimposed tissue associated with conventional mammography. In addition the increased volumetric information should enable temporal datasets to be more accurately compared, a task that radiologists routinely apply to conventional mammograms to detect the changes associated with malignancy. In this paper we address the problem of comparing DBT data by combining reconstruction of a pair of temporal volumes with their registration. Using a simple test object, and DBT simulations from in vivo breast compressions imaged using MRI, we demonstrate that this combined reconstruction and registration approach produces improvements in both the reconstructed volumes and the estimated transformation parameters when compared to performing the tasks sequentially.

1 Introduction

Digital breast tomosynthesis (DBT) is an X-ray modality in which a small number of low dose X-ray images (typically between 10 and 50) are acquired over a limited angle and reconstructed into a 3D volume[1]. The resulting images, which have high in-plane resolution but low out-of-plane resolution, exhibit reduced superposition of overlying tissue structures as compared to conventional X-ray mammography. Whilst the added depth information offered by DBT has the potential to enhance detection and diagnosis of breast cancer [2]; the greater volume of data, relative to X-ray mammography, increases the need for automated tools to aid the reading process. This is of particular importance if DBT is to be adopted in the high workload screening context.

†Contact Email: {g.yang, j.hipwell, s.arridge}@cs.ucl.ac.uk. This work has been funded by DTI Project *Digital Breast Tomosynthesis* TP/7/SEN/6/1/M1577G. The authors would like to thank the UK MR Breast Screening Study (MARIBS) for providing the data for this study.

In this paper we address the problem of comparison of temporal DBT volumes via registration. This is a challenging task due to the significant artefacts associated with DBT reconstructions. These are generated by the limited field of view of the acquired images and the correspondingly large null-space in the frequency domain. Rather than registering the images after reconstruction therefore, we investigate the benefits of combining both reconstruction and registration, and the hypothesis that the performance of each task will be enhanced as a result. In recent research on SPECT imaging [3] the authors present a method to combine reconstruction with motion correction using a rigid transformation. We have developed an iterative algorithm [4] which alternates between optimising the reconstructed intensities at each time point and the affine transformation parameters between time points.

2 Method

Two sets of limited angle X-ray acquisitions, $\vec{y}_1 \in \Re^{N_2}$ and $\vec{y}_2 \in \Re^{N_2}$, obtained at different times, can be expressed in terms of a 3D volume, $\vec{x} \in \Re^{N_3}$, in two positions related by the transformation, R, with parameters, $\vec{\zeta}_p \in \Re$, and the system matrix $A : \Re^{N_3} \mapsto \Re^{N_2}$ via

$$\vec{y}_1 = A\vec{x}, \tag{1}$$

$$\vec{y}_2 = A\vec{x}^{\dagger} = AR_{\vec{\zeta}_p}\vec{x}. \tag{2}$$

We solve equations 1 and 2 with respect to estimates $\vec{x}_1$ and $\vec{x}_2$ of $\vec{x}$ and the registration parameters $\vec{\zeta}_p$, by alternating an incomplete optimisation (*i.e.* n iterations) of the reconstructed volumes $\vec{x}_1$ and $\vec{x}_2$:

$$\vec{x}_1^* = \arg\min_{\vec{x}_1} \left(\Phi_{Rec1} = \frac{1}{2}\left\|A\vec{x}_1 - \vec{y}_1\right\|_2^2 \right) \tag{3}$$

$$\vec{x}_2^* = \arg\min_{\vec{x}_2} \left(\Phi_{Rec2} = \frac{1}{2}\left\|A\vec{x}_2 - \vec{y}_2\right\|_2^2 \right) \tag{4}$$

with the registration of the current estimates $\vec{x}_1^*$ and $\vec{x}_2^*$ with respect to the registration parameters $\vec{\zeta}_p$:

$$\zeta_p{}^* = \arg\min_{\vec{\zeta}_p} \left(\Phi_{Reg} = \frac{1}{2}\left\|R_{\vec{\zeta}_p}\vec{x}_2^* - \vec{x}_1^*\right\|_2^2 \right). \tag{5}$$

After each registration iteration (Eq. 5), and prior to the next iteration of the reconstructions (Eqs. 3 and 4), the reconstruction estimates are updated as follows (Eqs. 6 and 7). The last iteration outputs $\vec{x}_1 = \vec{x}_1^*$, $\vec{x}_2 = \vec{x}_2^*$ and $R_{\vec{\zeta}_p}\vec{x}_2^*$.

$$\vec{x}_1 = R_{\vec{\zeta}_p}\vec{x}_2^* \tag{6}$$

$$\vec{x}_2 = \vec{x}_2^*. \tag{7}$$

This "outer loop" of reconstruction followed by registration is repeated m times.

The reconstruction is performed via a nonlinear conjugate gradient search engine and the registration currently via a simple hill-climbing optimisation method. The following analytical gradients are used for $\vec{x}_1$ and $\vec{x}_2$

$$\Psi_{\vec{x}_1} = A^T(A\vec{x}_1 - \vec{y}_1) \tag{8}$$

$$\Psi_{\vec{x}_2} = A^T(A\vec{x}_2 - \vec{y}_2). \tag{9}$$

3 Results

In the following two experiments we compare the performance of (a) *sequential* reconstruction and registration, in which $n = 100$ iterations of the reconstruction of projection images, $\vec{y}_1$ and $\vec{y}_2$, are followed by a single registration of the reconstructed volumes $\vec{x}_1$ and $\vec{x}_2$ ($m = 1$) and (b) our *iterative* approach in which $n = 10$ iterations of the reconstruction are followed by a registration and the process is repeated $m = 10$ times. In both cases the total number of reconstruction iterations is the same ($m \times n = 100$). However, there are 10 registrations in our iterative method rather than one registration used in the sequential method. For each pair of test volumes, $\vec{x}$ and $\vec{x}^{\dagger}$, 11 projections covering ± 25 degrees are created to simulate the pair of temporal DBT acquisitions $\vec{y}_1$ and $\vec{y}_2$.

In the first experiment a 3D toroidal phantom image was created and a rigidly transformed one with $R_{\vec{\zeta}_p}$ equal to a translation of $T_{x,y,z} = [10, 0, -20]$ mm and a rotation about the y axis of -30 degrees (Fig. 1). As seen in Fig. 1. (f) and (h), the *iterative* results are more compact and accurate than the *sequential results* Fig. 1. (b) and (d), and the out of plane blurring is reduced (coloured squares). The sum of squared differences (SSD) $\|x_1 - x\|_2^2$ is decreased from 10^{11} to 10^9 in order of magnitude; however, for the *iterative* method this value of 4.32×10^9 is superior to the *sequential* result of 6.89×10^9.

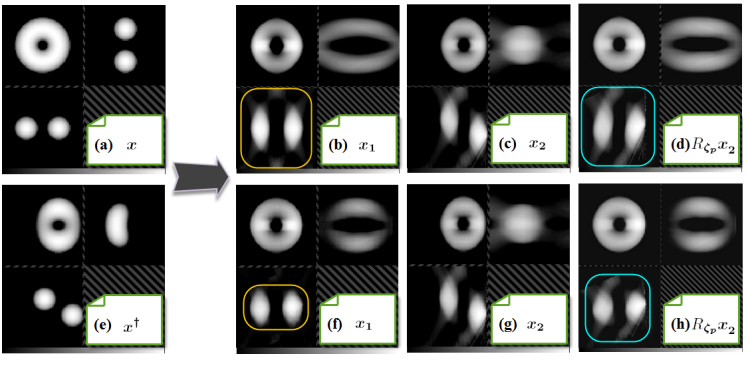

Figure 1: *(a) Original test volume $\vec{x}$; (e) Transformed test volume $\vec{x}^{\dagger}$; Sequential results (b)-(d): (b) reconstruction $\vec{x}_1$, (c) reconstruction $\vec{x}_2$, and (d) transformed reconstruction $R_{\vec{\zeta}_p}\vec{x}_2$; Iterative results (f)-(h): (f) reconstruction $\vec{x}_1$, (g) reconstruction $\vec{x}_2$, and (h) transformed reconstruction $R_{\vec{\zeta}_p}\vec{x}_2$.*

	Initial	Sequential Method	Combined Method
Toroid SSD	4.51×10^{11}	6.89×10^9	4.32×10^9
Compressed MRI SSD	6.91×10^{11}	7.60×10^9	5.90×10^9
Registration Error (mm)	23.6	8.6	4.6

Table 1: *Numerical results of the two experiments.*

In the second experiment we tested the methods using two MRI acquisitions obtained before and after application of a lateral-to-medial plate compression of the breast (Fig. 2). The SSD between reconstruction, $\vec{x}_1$, and the original volume, $\vec{x}$, indicates that the *iterative* method produces a more accurate reconstruction of the data (*iterative* 5.9×10^9 vs *sequential* 7.6×10^9 decreased from 6.91×10^{11}). In addition, measurement of the target registration error for a set of 12 user defined landmarks, indicates that the *iterative* method also produces a more

accurate registration result (4.6mm vs 8.6mm, given an initial misregistration of 23.6mm). All the numerical results of the two experiments above are shown in the Table 1.

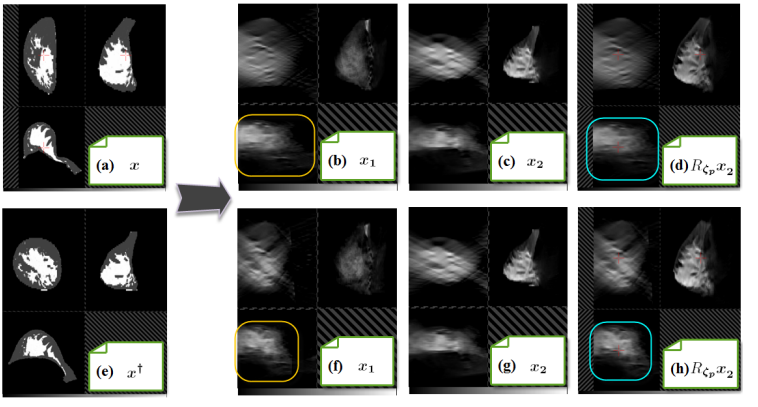

Figure 2: *As Fig. 1 but applied to in vivo MRI acquisition of a breast before and after plate compression (Images have been segmented and mapped to effective X-ray attenuation).*

Plots of the cost function $\Phi_{Rec1} = \|A\vec{x}_1 - \vec{y}_1\|_2^2$ represented in equation 3 for both sequential and combined methods are shown in Figures 3 and 4 following:

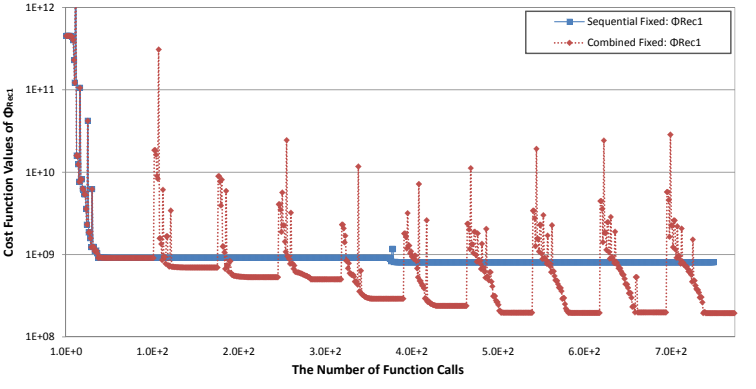

Figure 3: *Plot of the cost function $\Phi_{Rec1} = \|A\vec{x}_1 - \vec{y}_1\|_2^2$ for the 3D toroid experiment.*

4 Discussion and Conclusion

We have presented a method to iteratively reconstruct and register temporal DBT data sets and compared this approach with performing the two tasks sequentially.

Our iterative method was found to produce superior results in optimised cost function value, registration accuracy and reconstructed image appearance as seen in Fig. 5. We attribute this to the fact that the iterative approach uses all the X-ray acquisition data from both time points (y_1 and y_2) to reconstruct volume x_1.This leads to an improvement in the reconstruction of x_1 which in turn enables a more accurate registration to reconstructed volume x_2 to be achieved.

The iterative method updates reconstructed volume x_1 with the transformation of x_2 ($R_{\vec{\zeta}_p} \vec{x}_2^*$) following each registration iteration. This results in the 10 cost function peaks shown

in Fig. 3, rather than smoothly decreasing sequential graph. In addition, SSD has been used to take advantage of both mathematical simplicity and computational efficiency over other metrics such as the correlation coefficient and mutual information. Future work aims to test using real DBT data, non-rigid transformations, and alternative similarity metrics.

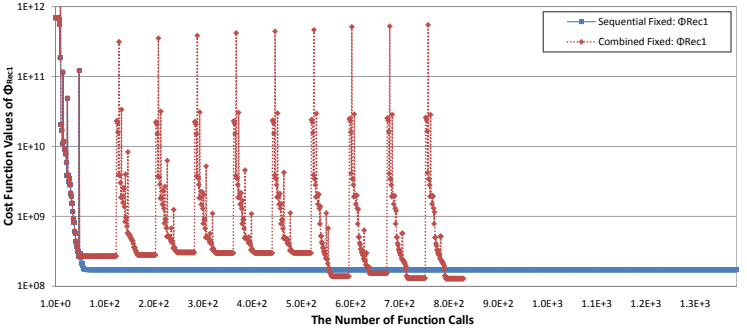

Figure 4: *As Fig. 3 but for the in vivo compressed MR experiment.*

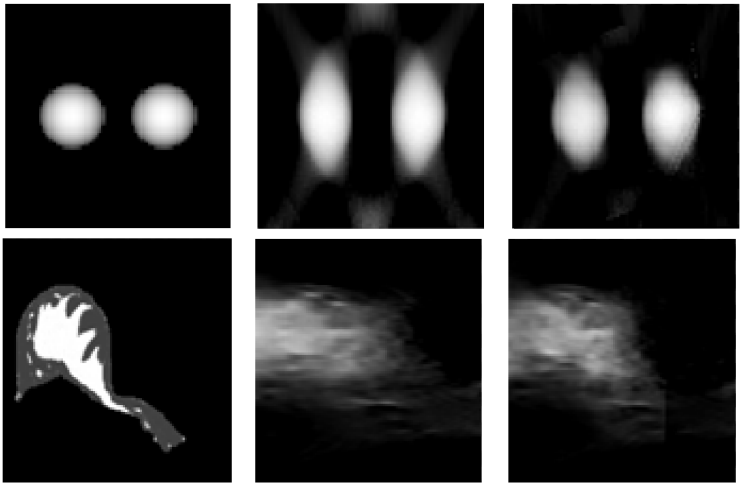

Figure 5: *Zoomed in results of the two tests above; (a), (b) and (f) of Figures 1 and 2. Left: Original fixed image x; Middle: Results of the sequential method x_1; Right: Results of the iterative method x_1. Only one view of each volume has been shown accordingly.*

References

[1] Wu, T., et al.: Tomographic Mammography Using a Limited Number of Low-dose Cone-beam Projection Images. Medical Physics 30, 365–380 (2003)

[2] Kopans, D.B.: Breast Imaging. 3rd Edition, Lippincott Williams and Wilkins, Philadelphia (2007)

[3] Schumacher, H., et al.: Combined Reconstruction and Motion Correction in SPECT Imaging. IEEE Transactions on Nuclear Science 56, 73–80 (2009)

[4] Yang, G., et al.: Combined Reconstruction and Registration of Digital Breast Tomosynthesis. IWDM'10: Proceedings of the 10th International Workshop on Digital Mammography. Lecture Notes in Computer Science 6136, Springer, 760–768 (2010)